



OPEN

CONFERENCE  
PROCEEDINGS

ACSMS2014

.....

SUBJECT AREAS:  
TWO-DIMENSIONAL  
MATERIALS

SYNTHESIS AND PROCESSING

Received  
29 August 2014Accepted  
31 October 2014Published  
3 December 2014

Correspondence and requests for materials should be addressed to L.H.L. (luhua.li@deakin.edu.au) or Y.C. (ian.chen@deakin.edu.au)

# High-Efficient Production of Boron Nitride Nanosheets via an Optimized Ball Milling Process for Lubrication in Oil

Deepika<sup>1,2</sup>, Lu Hua Li<sup>1</sup>, Alexey M. Glushenkov<sup>1,3</sup>, Samik K. Hait<sup>2</sup>, Peter Hodgson<sup>1</sup> & Ying Chen<sup>1</sup>

<sup>1</sup>Institute for Frontier Materials, Deakin University, Geelong Waurm Ponds Campus, Victoria 3216, Australia, <sup>2</sup>Indian Oil Corporation Limited, R&D Centre, Sector 13, Faridabad, Haryana 121007, India, <sup>3</sup>Melbourne Centre for Nanofabrication, 151 Wellington Rd, Clayton, VIC 3168, Australia.

Although tailored wet ball milling can be an efficient method to produce a large quantity of two-dimensional nanomaterials, such as boron nitride (BN) nanosheets, milling parameters including milling speed, ball-to-powder ratio, milling ball size and milling agent, are important for optimization of exfoliation efficiency and production yield. In this report, we systematically investigate the effects of different milling parameters on the production of BN nanosheets with benzyl benzoate being used as the milling agent. It is found that small balls of 0.1–0.2 mm in diameter are much more effective in exfoliating BN particles to BN nanosheets. Under the optimum condition, the production yield can be as high as 13.8% and the BN nanosheets are 0.5–1.5  $\mu\text{m}$  in diameter and a few nanometers thick and of relative high crystallinity and chemical purity. The lubrication properties of the BN nanosheets in base oil have also been studied. The tribological tests show that the BN nanosheets can greatly reduce the friction coefficient and wear scar diameter of the base oil.

Two-dimensional (2D) nanosheets including graphene, nanosheets of boron nitride (BN) and molybdenum disulphide ( $\text{MoS}_2$ ) have received intensive attention, because of their attractive mechanical<sup>1</sup>, thermal<sup>2</sup> and electronic properties<sup>3</sup>. BN nanosheets have many unique characteristics such as a wide bandgap, deep ultraviolet light emission<sup>4,5</sup>, high thermal stability<sup>6</sup>, controllable electrical conductivity<sup>7</sup> and unique wettability<sup>8,9</sup>. BN is also considered as a green lubricant which can be used in engine oil at high temperatures<sup>10</sup>. Similar to other 2D materials, BN nanosheets can be produced in either a bottom-up or top-down manner. The bottom-up method includes chemical vapor deposition<sup>11–13</sup> and segregation method<sup>14</sup>; the top-down method is exfoliating bulk hBN crystals via mechanical<sup>15–17</sup> or sonication methods<sup>18–20</sup>. It has been demonstrated that tailored wet ball milling is an efficient and high-yield method to produce atomically thin BN nanosheets of high crystallinity<sup>16,17</sup>. Among water, ethanol, dodecane and benzyl benzoate milling agents, benzyl benzoate gives the best peeling results due to its relatively high density and similar surface energy to hBN. The peeling efficiency or nanosheet yield by ball milling can also closely relate to many other milling parameters, such as ball size, milling speed and ball-to-powder ratio which have not been investigated. Here, we systematically studied these parameters for optimized production of large quantities of BN nanosheets in benzyl benzoate by ball milling. The lubricating properties of the BN nanosheets in base oil were also tested.

## Results and Discussion

**Milling time effect.** The starting hBN particles have a typical disc-like shape with diameters of 10–20  $\mu\text{m}$  and thickness in the order of 100 nm, as shown by the scanning electron microscopy (SEM) image in Figure 1a. Different from traditional ball milling technique which normally causes dramatic damage to the sample<sup>21–23</sup>, ball milling in a liquid agent was chosen to reduce impact. The study of milling time effect on BN peeling was based on 1 mm steel balls with a ball-to-powder weight ratio of 10:1 at a milling speed of 800 rpm in benzyl benzoate. According to SEM studies, most of the hBN particles become delaminated after 2 h milling. Figure 1b and c show partially exfoliated hBN particles caused by the impact of the milling balls which predominantly produced shear force during the milling. Under the shearing force, the weak interplanar bonds broke and thinner BN sheets could be produced. However, the yield of few-layer BN was still low at this stage (2 h). With the extension of milling time to 5 h, the exfoliation was more complete, as shown in Figure 1d that there were more BN nanosheets than hBN particles. After 10 h milling, the yield of BN nanosheets further increased, but the size of the BN nanosheets

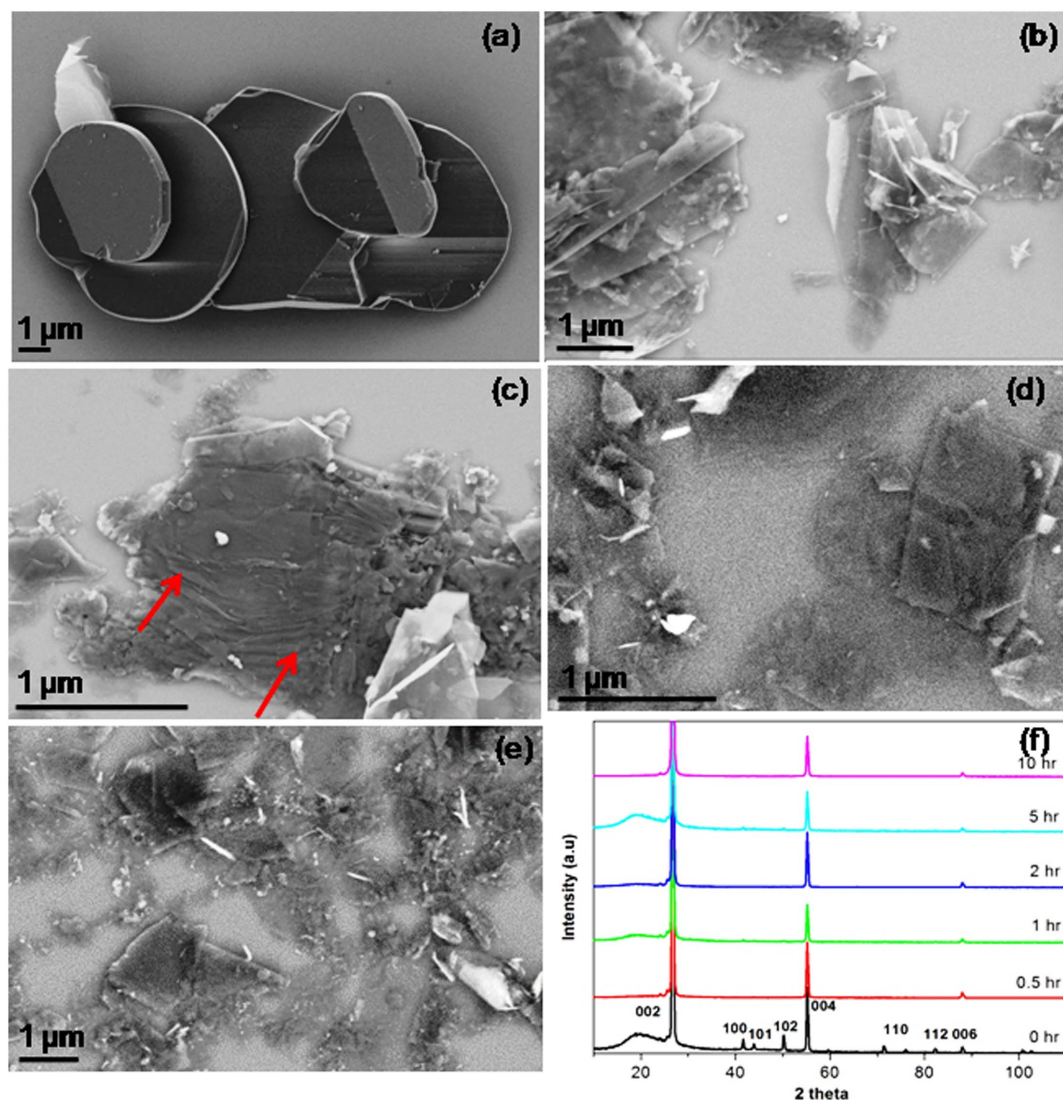


**Figure 1** | SEM images of (a) starting hBN particles; (b, c) partially exfoliated hBN particles after 2 h milling; (d) more exfoliated particles after 5 h milling; (e) completely exfoliated particles after 10 h milling; and (f) normalized XRD spectra of the initial hBN particles and the sheets ball milled for different periods of time without centrifugation.

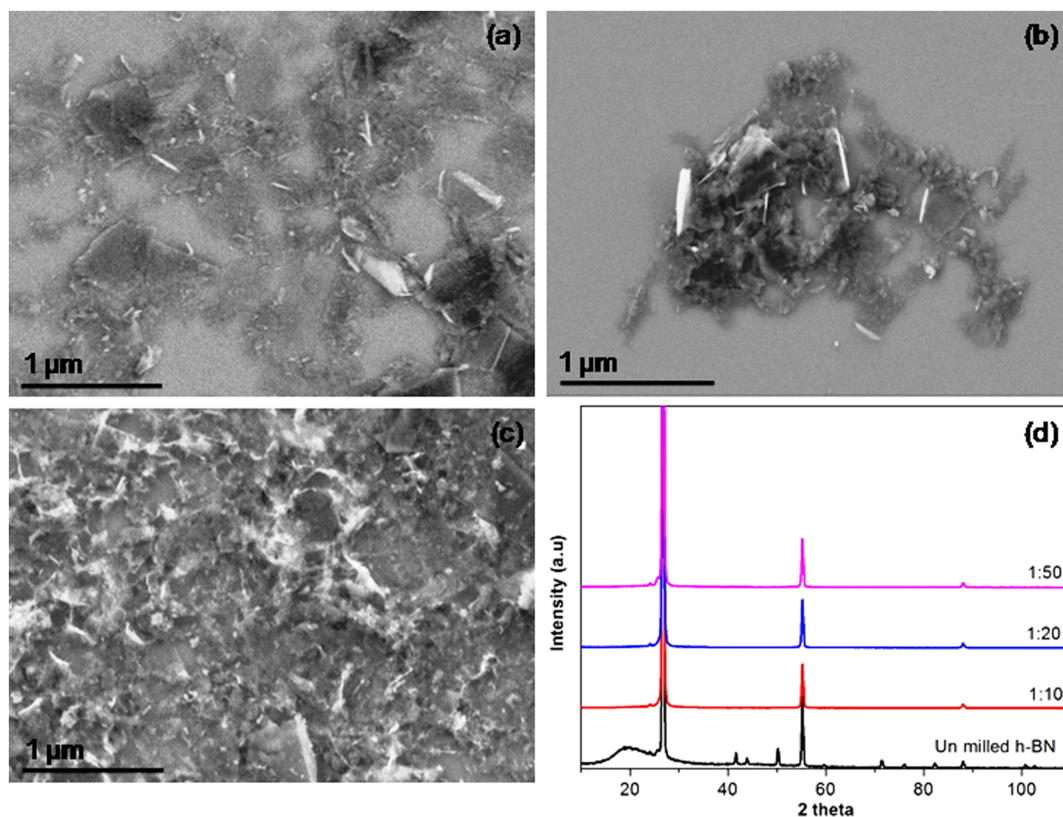
slightly reduced compared to the product from the 5 h milling. This indicates that certain milling time is required to allow the full exfoliation of BN, but extended milling should be avoided to minimize damage to the BN nanosheets. In this particular case, the best milling time is 10 h.

Figure 1f shows the normalized X-ray diffraction (XRD) spectra of the BN milled for different periods of time. The starting particles show a typical XRD spectrum of hBN with strong (002) and (004) peaks. Even after 10 h milling, the relative intensities of the (004) and (006) peaks only slightly decrease and there is no measurable broadening of the (002), (004) and (006) peaks. These suggest that the milling has a small impact on the in-plane structure of BN. The (100), (101), (102), (110) and (112) peaks, in contrast, almost disappear after 0.5 h milling, which is caused by the preferential orientation of the milled BN on substrate due to their reduced thickness-to-size ratio. In other words, the milling effectively exfoliates hBN particles to BN nanosheets.

**Ball-to-powder ratio effect.** The milling effect of various ball-to-powder weight ratios were investigated using 1 mm steel balls for milling time of 10 h. Compared to the results from the ball-to-powder ratio of 10:1, a similar amount of BN nanosheets were produced when the ratio increased to 20:1 (Figure 2a). However,

the 20:1 ratio produced more BN nanosheets less than 200 nm in diameter. When the 50:1 ratio was applied, many small particles instead of sheets were found. The formation of these particles are due to damage to the BN nanosheets<sup>20</sup>. This indicates that the increase of ball-to-powder ratio can result in higher yields of sheets, but at the cost of more structural damage owing to higher chance of ball-to-vial or ball-to-ball collision and also possibly stronger collision. The XRD patterns of samples milled with the different ball ratios are similar, and there is no noticeable broadening of the (002) and (004) peaks for all three samples (Figure 2c). Therefore, the ideal ball-to-powder ratio is 10:1.

**Milling speed effect.** Milling speed is another important parameter. The milling speed was reduced to 600 rpm with the above optimized conditions (milling time of 10 h and ball-to-powder ratio of 10:1). The amount of BN nanosheets produced at 600 rpm is close to that produced at 800 rpm, but the 600 rpm produced sheets are thicker and larger in size (Fig. 3a) due to the smaller shear force created by the balls and hence less exfoliation. The XRD characterization (Figure 3b) reveals that the intensities of (004) and (006) peaks decrease with the increase of milling speed, suggesting more change to the c-direction of the BN crystal and therefore more



**Figure 2** | SEM images for sample ball milled with different ball-to-powder ratio (a) 10:1, (b) 20:1, (c) 50:1 and (d) normalized XRD spectra of the initial hBN particles and the sheets ball milled with different ball-to-powder ratio without centrifugation.

thickness reduction. In addition, the (100), (101) and (102) peaks are still visible after 600 rpm milling whereas these peaks disappear for the sample milled at 800 rpm. This indicates that the 600 rpm milled sheets have a smaller size-to-thickness ratio and hence less effective exfoliation.

**Ball size effect.** The effect of ball size (1.0, 0.6–0.8 and 0.1–0.2 mm) on the extent of exfoliation was also studied by keeping other milling parameters the same (milling time of 10 h, ball-to-powder ratio of 10:1 and speed of 800 rpm). SEM analyses reveal that the 0.6–0.8 mm balls produce similar amounts of BN nanosheets (Figure 4b). However, when the 0.1–0.2 mm balls are used, the yield of BN nanosheets dramatically increases and their thickness

is smaller and more homogeneous (Figure 4a and c). The size of the BN nanosheets produced by the 0.1–0.2 mm balls is estimated from the SEM images and about 1/3 of the nanosheets has a diameter less than 1  $\mu\text{m}$  and about 2/3 is between 1.0 and 1.5  $\mu\text{m}$  (see Supplementary Information, Figure S2). This result is not surprising by considering the more surface area and lighter in weight of the 0.1–0.2 mm balls compared to those of the 0.6–0.8 and 1.0 mm balls. The larger surface area can create more chance of ball-to-ball or ball-to-vial interaction/impact and therefore more shearing on the BN crystals. Their lighter weight makes the shear force gentler so that damage on BN nanosheets can be minimized. The XRD patterns from the samples produced by balls of different sizes are compared in Figure 4d. The Raman spectrum of the BN

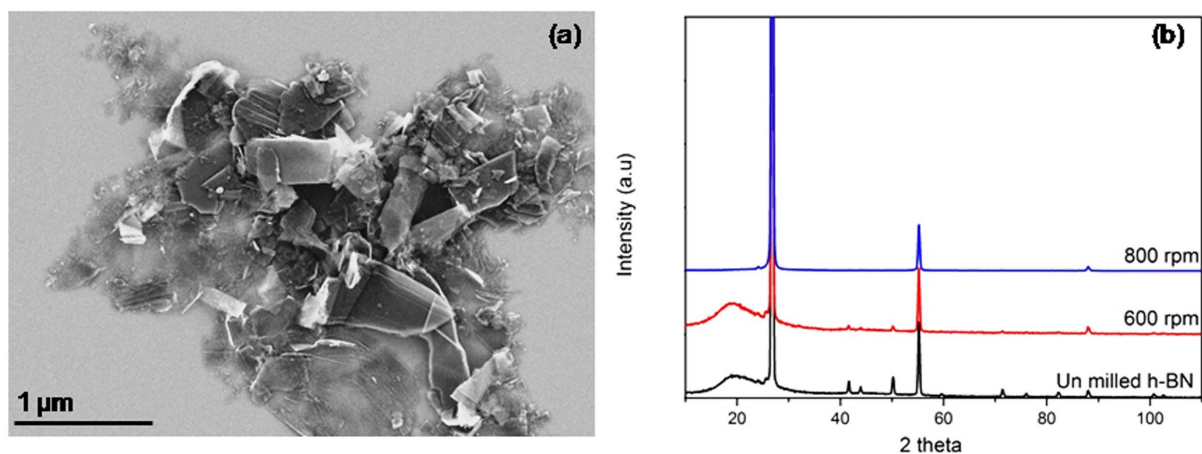


**Figure 3** | SEM image of the sample ball milled at 600 rpm; (b) normalized XRD spectra of the initial hBN particles and the nanosheets ball milled at different milling speeds without centrifugation.



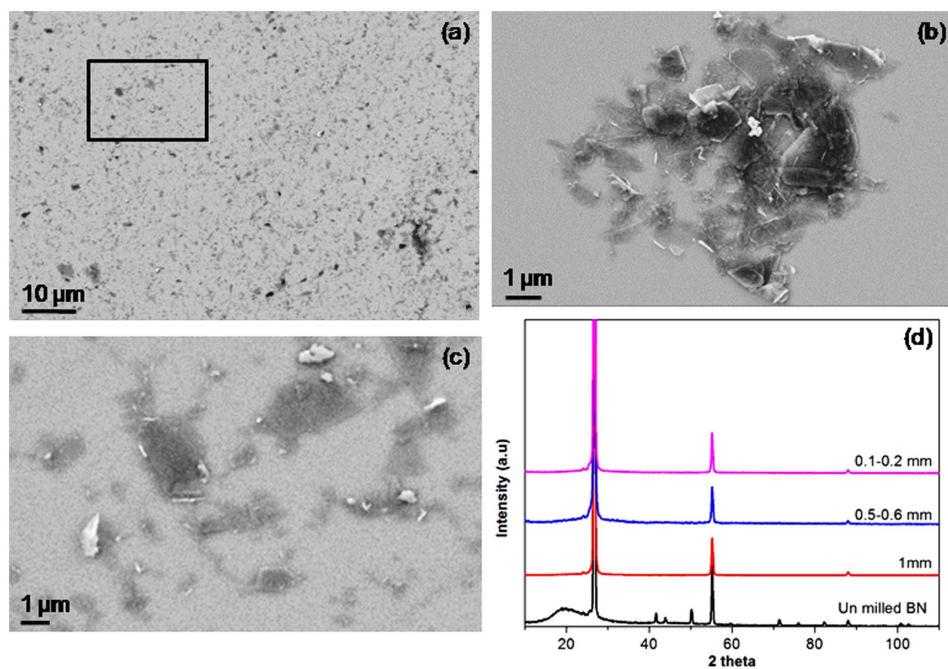


**Figure 4** | SEM images of the sample ball milled with different ball sizes (a) 0.1–0.2 mm (b) 0.6–0.8 mm, (c) higher magnification of selected area (indicated as box) from image “a”, and (d) normalized XRD spectra of the initial hBN particles and the sheets ball milled with different ball sizes without centrifugation.

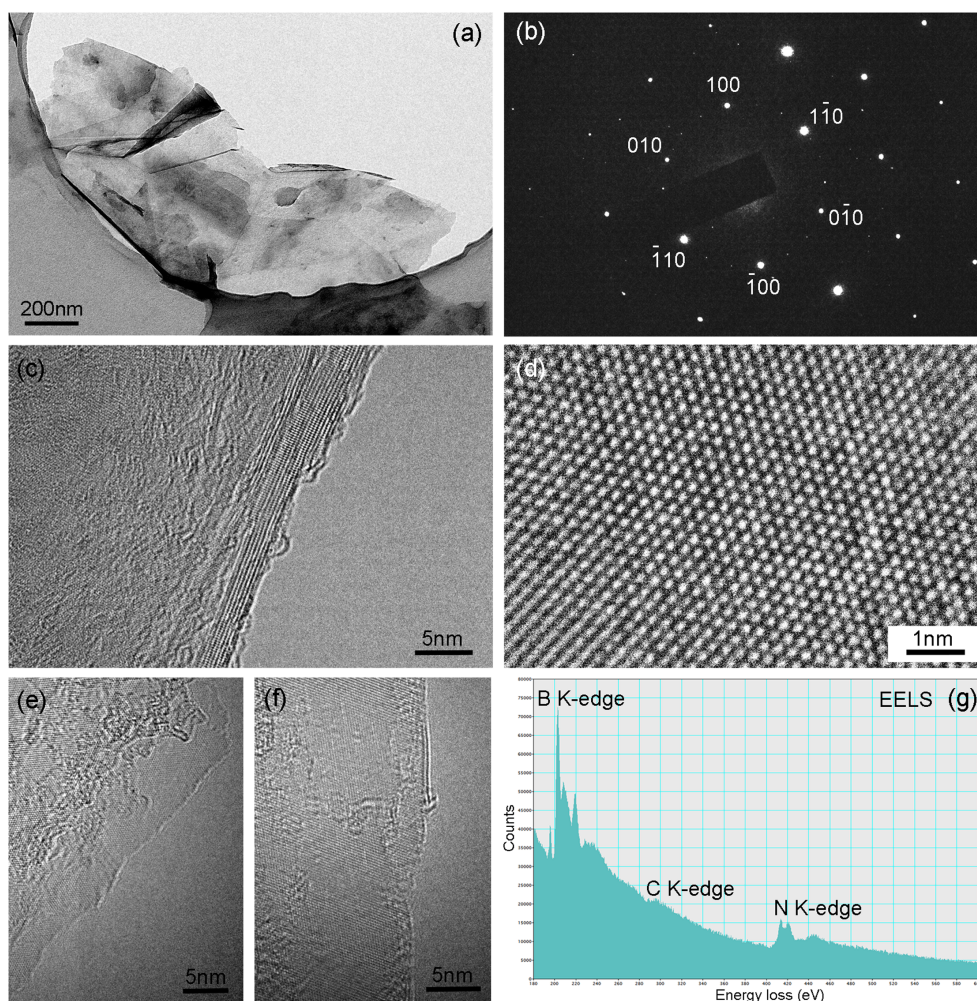


**Figure 5** | (a) TEM Images of the BN sheets produced by 0.1–0.2 mm balls; (b) the corresponding SAED pattern; (c) and (d) high-magnification TEM images; (e) and (f) TEM images of few-layer BN nanosheets (g) EELS spectra of the BN nanosheet.



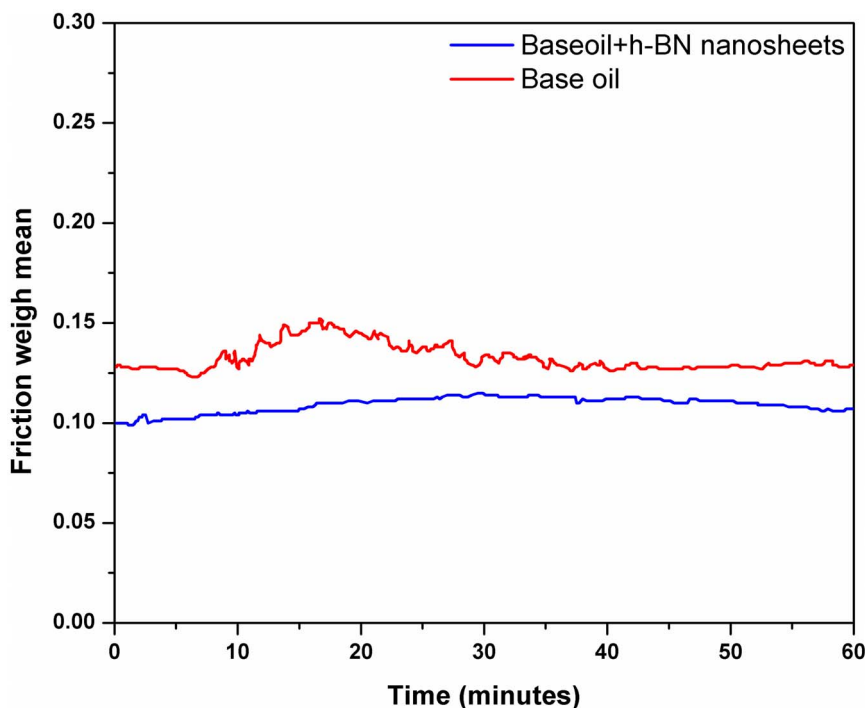


**Figure 6** | Coefficient of friction at fixed load and constant temperature for neat base oil (red) and base oil containing BN nanosheets (blue).

produced using the 0.1–0.2 mm balls is shown in the Supplementary Information (Figure S1).

To confirm that the 0.1–0.2 mm balls give the best exfoliation, we estimated the production yield of all above mentioned samples using different milling conditions. It is the 0.1–0.2 mm balls with 800 rpm and ball-to-powder ratio of 10 : 1 that give rise to the highest yield of 13.8%. The milling with 0.1–0.2 mm balls at 600 rpm has slightly lower yield of 13.0%. These yield values are several times larger than those using the 1.0 and 0.6–0.8 mm balls.

The crystallinity, thickness and chemical composition of the BN nanosheets produced by ball milling using the 0.1–0.2 mm balls were investigated by transmission electron microscopy (TEM) and electron energy loss spectroscopy (EELS). Figure 5a shows a BN nanosheet suspended over a holey carbon supporting film on a TEM grid. Similar to many other investigated BN nanosheets, folds and partial exfoliation are observed. The electron diffraction pattern in Figure 5b shows one set of bright dots and several sets of weaker dots both of a six-fold symmetry. This suggests that the BN nanosheet is still crystalline and the in-plane structure is not damaged, consistent with the XRD results. However, the presence of the sets of weaker diffraction dots discloses that either the stacking of the BN nanosheet is twisted or the existence of folds or incomplete exfoliation. High-

resolution TEM image in Figure 5c show the edge of part of the BN nanosheet, indicating a thickness of 2 nm (~6 layers). The highly crystalline nature of the BN nanosheet is confirmed by the HRTEM image in Figure 5d, showing a pattern of lattice dots with a distance of 0.25 nm representing the distance between two adjacent BN hexagonal rings. So the distance between B and N atoms is calculated to be 0.144 nm, typical for hBN crystals. We also found few-layer BN, as shown in Figure 5e and f. The EELS spectrum in Fig. 5g shows the domination of B and N, along with a small amount of carbon. The carbon could come from the residue of benzyl benzoate which is not fully evaporated during TEM sample preparation.

**Tribology studies.** The tribological properties of the BN nanosheets produced under the optimum ball milling condition, i.e. ball milling at 800 rpm using 0.1–0.2 mm balls at a ball-to-powder ratio of 10 : 1 for 10 h, were tested. Figure 6 shows the plot of friction of coefficient versus time of neat base oil and base oil containing BN nanosheets. The oil containing BN nanosheets shows smaller friction compared to the neat oil. The drop in friction could be due to the alignment of nanosheets on metal surface parallel to the direction of motion<sup>24</sup>. Figure 7 shows the SEM images of worn surfaces of the stationary balls used for testing the neat base oil and base oil containing BN nanosheets. The neat base oil

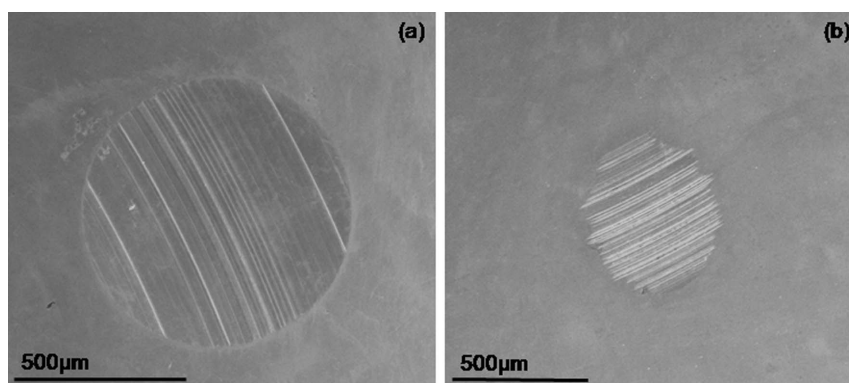


**Figure 7** | SEM images of worn-surfaces of the stationary balls tested for (a) neat base oil and (b) base oil with BN nanosheets.



gives the biggest scar of around 1 mm; while the BN nanosheet blended base oil shows remarkable reduction in wear scar diameter (0.5 mm). This reduction in wear scar can be attributed to the good antiwear property of BN nanosheets. Several mechanisms, including the ball bearing effect, a protective film, the mending effect and the polishing effect, have been invoked to explain the friction reduction enhancement in lubricants containing nanoparticles<sup>25</sup>. The mending effect mechanism is considered to be valid in our case, because of the layered structure and flexibility of BN nanosheets<sup>26</sup>.

## Conclusions

Wet ball milling is highly efficient in BN nanosheet production with little damage to the in-plane structure. Milling time, ball-to-powder ratio, milling speed and ball size all play important roles for achieving a high yield. Under the optimized milling condition and with benzyl benzoate as the milling agent, the production yield is about 13.8% and the BN nanosheets have sizes of 0.5–1 μm and thicknesses of a few nanometers. The resultant BN nanosheets are of relative high crystallinity and chemical purity. The synthesized BN nanosheets can reduce the wear scar and coefficient of friction of base oil in four-ball tests, which suggests that BN nanosheets can give substantial improvements in lubrication.

## Methods

A typical amount (0.5 g) of hBN powder (PT110, Momentive) and 10 mL benzyl benzoate (purity ≥ 99%, Sigma-Aldrich) were milled in a horizontal planetary ball mill (Pulverisette 7, Fritsch) using steel vials. Milling balls of different sizes were tested: 1.0 mm (steel), 0.6–0.8 mm and 0.1–0.2 mm (both Zr<sub>2</sub>SiO<sub>4</sub>). Vials were sealed and filled with argon (Ar) gas at a pressure of 200 kPa above the atmospheric pressure to avoid environmental contamination. The milling speed was varied (600 and 800 rpm) with different powder to ball ratios (1 : 10, 1 : 20 and 1 : 50) for up to 10 h. At different time intervals (0.5, 1, 2, 5 and 10 h), small amounts of sample were removed from the vials for analysis.

XRD studies were carried out using a Pan-analytical Xpert Pro equipped with a copper anode. Samples for XRD were prepared by displacing samples directly taken out of the milling vial (without sonication and centrifugation) on glass substrates. SEM studies were conducted on a Zeiss Supra 55VP operated at 3 kV. For SEM analysis, samples were diluted with benzyl benzoate and bath sonicated for 15 minutes followed by centrifugation at 800 g (Eppendorf 5424 and 5430) to remove big BN particles. Then the samples were deposited on Si wafers and heated at 290 °C in air to remove benzyl benzoate. TEM studies were performed on a JEOL 2100F operated at 200 kV. The chemical composition was analyzed by EELS (Quantum, Gatan) under both TEM and scanning transmission electron microscope (STEM) modes.

To estimate the production yield of nanosheets, ball milled samples (2–3 mL) were mixed with benzyl benzoate (5–10 mL) followed by bath sonication for 15 minutes and centrifugation at 800 g for 1 h. The supernatant containing nanosheets was separated from the settled big particles. Supernatant and settled particles were filtered over membrane (0.45 μm pore sized) with the help of vacuum pump. Membrane containing nanosheets and big particles were dried and weighed to calculate the percentage yield:

$$\text{Percentage yield} = \frac{\text{Weight of nanosheets}}{\text{Total weight}} \times 100\%$$

Total weight is the weight of BN nanosheets and big BN particles.

In the tribological studies, the BN nanosheets produced by ball milling were dispersed in group-II base oil at 0.01 wt.% by ultrasonication without the use of any surfactant, dispersant or chemical material. The friction-reduction was examined using an Optimol SRV oscillating friction under 50 N load at 50 °C for 1 h. AW properties were examined using a four-ball wear tester (Falex) under 15 kg load at 75 °C and 1200 rpm for 1 h. After wear tests, all the specimens were carefully cleaned with petroleum ether and followed by SEM analysis conducted on a Hitachi S-3400N instrument under an accelerating voltage of 15 kV. All the above measurements were performed for three times and best of the two were taken for evaluation.

- Lee, C., Wei, X., Kysar, J. W. & Hone, J. Measurement of the elastic properties and intrinsic strength of monolayer graphene. *Science* **321**, 385–388 (2008).
- Balandin, A. A. *et al.* Superior thermal conductivity of single-layer graphene. *Nano Lett.* **8**, 902–907 (2008).
- Novoselov, K. S. *et al.* Two-dimensional gas of massless Dirac fermions in graphene. *Nature* **438**, 197–200 (2005).
- Li, L. H. *et al.* Photoluminescence of boron nitride nanosheets exfoliated by ball milling. *Appl. Phys. Lett.* **100**, 261108 (2012).
- Li, L. *et al.* High-quality boron nitride nanoribbons: Unzipping during nanotube synthesis. *Angew. Chem. Int. Ed.* **52**, 4212–4216 (2013).

- Li, L. H., Cervenkova, J., Watanabe, K., Taniguchi, T. & Chen, Y. Strong oxidation resistance of atomically thin boron nitride nanosheets. *ACS Nano* **8**, 1457–1462 (2014).
- Zeng, H. B. *et al.* “White graphemes”: Boron nitride nanoribbons via boron nitride nanotube unwrapping. *Nano Lett.* **10**, 5049–5055 (2010).
- Pakdel, A., Zhi, C. Y., Bando, Y., Nakayama, T. & Golberg, D. Boron nitride nanosheet coatings with controllable water repellency. *ACS Nano* **5**, 6507–6515 (2011).
- Li, L. H. & Chen, Y. Superhydrophobic properties of nonaligned boron nitride nanotube films. *Langmuir* **26**, 5135–5140 (2010).
- Taha-Tijerina, J. *et al.* Electrically insulating thermal nano-oils using 2D fillers. *ACS Nano* **6**, 1214–1220 (2012).
- Shi, Y. *et al.* Synthesis of few-layer hexagonal boron nitride thin film by chemical vapor deposition. *Nano Lett.* **10**, 4134–4139 (2010).
- Song, L. *et al.* Large scale growth and characterization of atomic hexagonal boron nitride layers. *Nano Lett.* **10**, 3209–3215 (2010).
- Yu, J. *et al.* Vertically aligned boron nitride nanosheets: Chemical vapor synthesis, ultraviolet light emission, and superhydrophobicity. *ACS Nano* **4**, 414–422 (2010).
- Xu, M. S., Fujita, D., Chen, H. Z. & Hanagata, N. Formation of monolayer and few-layer hexagonal boron nitride nanosheets via surface segregation. *Nanoscale* **3**, 2854–2858 (2011).
- Pacile, D., Meyer, J. C., Girit, C. O. & Zettl, A. The two-dimensional phase of boron nitride: Few-atomic-layer sheets and suspended membranes. *Appl. Phys. Lett.* **92**, 133107 (2008).
- Li, L. H. *et al.* Large-scale mechanical peeling of boron nitride nanosheets by low-energy ball milling. *J. Mater. Chem.* **21**, 11862–11866 (2011).
- Liu, L. *et al.* Solid exfoliation of hexagonal boron nitride crystals for the synthesis of few-layer boron nitride nanosheets. *Chem. Lett.* **42**, 1415–1416 (2013).
- Lin, Y., Williams, T. V. & Connell, J. W. Soluble, exfoliated hexagonal boron nitride nanosheets. *J. Phys. Chem. Lett.* **1**, 277–283 (2009).
- Zhi, C., Bando, Y., Tang, C., Kuwahara, H. & Golberg, D. Large-scale fabrication of boron nitride nanosheets and their utilization in polymeric composites with improved thermal and mechanical properties. *Adv. Mater.* **21**, 2889–2893 (2009).
- Warner, J. H., Rummeli, M. H., Bachmatiuk, A. & Büchner, B. Atomic resolution imaging and topography of boron nitride sheets produced by chemical exfoliation. *ACS Nano* **4**, 1299–1304 (2010).
- Li, L. H., Chen, Y. & Glushenkov, A. M. Boron nitride nanotube films grown from boron ink painting. *J. Mater. Chem.* **20**, 9679–9683 (2010).
- Li, L. H., Chen, Y. & Glushenkov, A. M. Synthesis of boron nitride nanotubes by boron ink annealing. *Nanotechnology* **21**, 105601 (2010).
- Li, L. *et al.* Mechanically activated catalyst mixing for high-yield boron nitride nanotube growth. *Nanoscale Res. Lett.* **7**, 417 (2012).
- Pawlak, Z., Kaldonski, T., Pai, R., Bayraktar, E. & Oloyede, A. A comparative study on the tribological behaviour of hexagonal boron nitride (h-BN) as lubricating micro-particles—an additive in porous sliding bearings for a car clutch. *Wear* **267**, 1198–1202 (2009).
- Lee, K. *et al.* Understanding the role of nanoparticles in nano-oil lubrication. *Tribol. Lett.* **35**, 127–131 (2009).
- Cho, D. H., Kim, J. S., Kwon, S. H., Lee, C. & Lee, Y. Z. Evaluation of hexagonal boron nitride nano-sheets as a lubricant additive in water. *Wear* **302**, 981–986 (2013).

## Acknowledgments

L.H.L. thanks Alfred Deakin Postdoctoral Research Fellowship for the financial support.

## Author contributions

L.H.L. and Y.C. designed the research; D. produced the material, did part of the characterization; L.H.L. and A.M.G. did the TEM analysis; D. and S.K.H. conducted the friction tests; P.H. involved in data analysis and result discussion. D. and L.H.L. co-wrote the manuscript with input from all the other authors.

## Additional information

Supplementary information accompanies this paper at <http://www.nature.com/scientificreports>

Competing financial interests: The authors declare no competing financial interests.

How to cite this article: Deepika. *et al.* High-Efficient Production of Boron Nitride Nanosheets via an Optimized Ball Milling Process for Lubrication in Oil. *Sci. Rep.* **4**, 7288; DOI:10.1038/srep07288 (2014).



This work is licensed under a Creative Commons Attribution-NonCommercial-ShareAlike 4.0 International License. The images or other third party material in this article are included in the article's Creative Commons license, unless indicated otherwise in the credit line; if the material is not included under the Creative Commons license, users will need to obtain permission from the license holder in order to reproduce the material. To view a copy of this license, visit <http://creativecommons.org/licenses/by-nc-sa/4.0/>